ZnO Nanocrystallites/Cellulose Hybrid Nanofibers Fabricated by Electrospinning and Solvothermal Techniques and Their Photocatalytic Activity

Shuhai Ye,[1] Dong Zhang,[1] Haiqing Liu,[1,2] Jinping Zhou[3]

[1]*College of Chemistry and Materials Science, Fujian Normal University, Fuzhou 350007, China*
[2]*Fujian Key Laboratory of Polymer Materials, Fuzhou 350007, China*
[3]*College of Chemistry and Molecular Science, Wuhan University, Wuhan 430072*

Received 28 March 2010; accepted 23 November 2010
DOI 10.1002/app.33822
Published online 4 March 2011 in Wiley Online Library (wileyonlinelibrary.com).

ABSTRACT: ZnO nanocrystallites have been *in situ* embedded in cellulose nanofibers by a novel method that combines electrospinning and solvothermal techniques. $Zn(OAc)_2$/cellulose acetate (CA) precursor hybrid nanofibers with diameter in the range of 160–330 nm were first fabricated via the electrospinning technique using zinc acetate as precursor, CA as the carrier, and dimethylformamide (DMF)/acetone(2 : 1) mixture as cosolvent. The precursor nanofibers were transformed into ZnO/cellulose hybrid fibers by hydrolysis in 0.1 mol/L NaOH aqueous solution. Subsequently, these hybrid fibers were further solvothermally treated in 180°C glycerol oil bath to improve the crystallite structure of the ZnO nanoparticles containing in the nanofibers. The structure and morphology of nanofibers were characterized by scanning electron microscopy, transmission electron microscopy, and X-ray diffraction. It was found that hexagonal structured ZnO nanocrystallites with the size of ~ 30 nm were dispersed on the nanofiber surfaces and within the nanofibers with diameter of about 80 nm. The photocatalytic property of the ZnO/cellulose hybrid nanofibers toward Rhodamine (RhB) was tested under the irradiation of visible light. As a catalyst, it inherits not only the photocatalytic ability of nano-ZnO, but also the thermal stability, good mechanical property, and solvent-resistibility of cellulose nanofibers. The key advantages of this hybrid nanofiber over neat ZnO nanoparticles are its elasticity, dimensional stability, durability, and easy recyclability. © 2011 Wiley Periodicals, Inc. J Appl Polym Sci 121: 1757–1764, 2011

Key words: electrospinning; hybrid; photocatalyst; solvothermal method

INTRODUCTION

The synthesis of polymeric nanofibers containing dispersed functional inorganic nanoparticles has attracted substantial research interest in recent years due to their potential applications in the areas of catalyst, electronic nanodevice, optoelectronic, sensor, and nanocomposite.[1–8] Distinct from the conventional polymer nanocomposites in the forms of film or bulky fiber, the physical size of the host polymer matrix and embedded particles of these inorganic/organic hybrid nanofibers are both in the submicrometer or nanometer range, thus the characteristic large surface areas of nanofibers and nanoparticles is retained.[1,9] Moreover, these hybrid nanofibers have been proved to possess both the advantages of organic polymers such as light weight, flexibility and moldability, and of inorganic species such as special functionality, high strength and thermal-stability.[10–12] For instance, the carbon nanotube (CNT)/polyacrylonitrile,[13] graphite nanoplatelet/polyacrylonitrile[6] hybrid nanofibers showed improved either electrical conductivity, mechanical properties, thermal stability, or dimensional stability. A straightforward approach in the fabrication of such hybrid nanofibers is through the electrospinning of polymer solutions with dispersed inorganic nanoparticles.[14–17] Another effective method is through sol–gel process to embed inorganic nanoparticles in nanofibers, such as zinc acetate/poly(vinyl alcohol)[18] and TiO_2/poly(vinyl pyrrolidone) nanofibers.[19–21] From the latter method, the inorganic nanoparticles impregnated in as-obtained hybrid nanofibers usually do not show special functionalities because the desired crystal structures of inorganic particles can not form at ambient processing temperature.[22,23] Therefore, hybrid nanofibers from the latter method are often calcinated at high temperature to completely remove the organic fiber template and to leave functional polycrystalline metal oxide nanofibers behind. Although the

Correspondence to: H. Liu (haiqing.liu@gmail.com).
Contract grant sponsor: National Natural Science Foundation of China; contract grant numbers: 50973019, 50843030.
Contract grant sponsor: National Basic Research Program of China; contract grant number: 2010CB732203.
Contract grant sponsor: Natural Science Foundation of Fujian Province; contract grant number: 2010J06017.

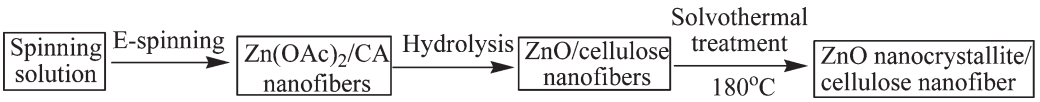

Scheme 1 Preparation procedure of the ZnO nanocrystallite/cellulose hybrid nanofibers.

resultant metal oxide nanofibers are very useful as electronic devices, optoelectronic materials and photocatalysts, they are fragile and readily to break into rod-like nanoparticles.[24] Thus the practical applications of pure metal oxide nanofibers are limited. To overcome this problem, *in situ* growth of metal oxide nanoparticles in polymeric nanofibers followed by proper treatments is a feasible solution. Hong et al. reported the preparation of poly(vinyl alcohol) (PVA) nanofibers with surface-residing ZnO nanoparticles.[25] However, the nano-ZnO/PVA hybrid nanofibers synthesized at ambient temperature did not show satisfied crystal structure, and the water solubility of the host PVA nanofiber matrix would prevent their applications in aqueous environment.

In this work, we introduce a new technique to prepare elastic nano-ZnO/cellulose hybrid nanofibers through the combination of electrospinning and solvothermal methods. Nano-ZnO is a functional material with many applications in fields of gas sensors, photocatalyst and optical devices.[26,27] Cellulose is selected as the host polymer nanofiber mainly due to its insolubility in many ordinary solvents and good thermal stability. The purpose is to obtain durable and recyclable photocatalytic hybrid nanofibers.[28] To this end, precursor zinc acetate (ZnAc) and fiber template polymer cellulose acetate (CA) are mixed in a common solvent, followed by electrospinning to produce submicron ZnAc/CA hybrid nanofibers. Subsequently, they are hydrolyzed in mild base solution to generate ZnO/cellulose hybrid nanofibers. As-obtained hybrid nanofibers are then solvothermally treated in glycerol at 180°C to convert them to crystal nano-ZnO/cellulose nanofibers for predetermined time. Their structures and morphologies are characterized by scanning electron microscopy (SEM), transmission electron microscopy (TEM), and X-ray diffraction (XRD). Their photocatalytic efficiency toward Rohdamine (RhB) is evaluated under the irradiation of visible light.

EXPERIMENTAL

Materials

Zinc acetate (ZnAc) dihydrate (Sinopharm Chemical Reagents, China) was recrystallized in distilled water to remove small content of impurities. CA with degree of substitution (DS) of 2.45 and M_w of 3.0×10^4 was obtained from Eastman, USA. *N*,*N*-dimethylformaide (DMF)/acetone and acetone (Sinopharm Chemical Reagents, China) of analytical grade were used as received.

Preparation of hybrid nanofibers

Transparent spinning solutions containing 4 wt % ZnAc were prepared by adding ZnAc into 20 wt % CA in 2 : 1 (v/v) DMF/acetone solvent mixture, followed by magnetic stirring at ambient temperature. They were placed in a syringe with a stainless needle of gauge 18. The feeding rate was 5 μL/min monitored by a syringe pump (TS2-60, Longer Precision Pump, Baoding, China). An electrode was clamped on the needle and connected to a power supply (DW-P303-IAC, Tianjin Dongwen High Voltage Plant, China). Grounded counter electrode was connected to collector aluminum foil, which was placed 10 cm away from the needle tip. The electric field was kept at 15 kV. The ZnAc/CA hybrid nanofibrous mats were dried in a vacuum oven at 90°C for 5 h.

The as-obtained hybrid nanofibrous mats were hydrolyzed in 0.1 mol/L NaOH aqueous solution for 24 h at ambient temperature to turn ZnAc/CA hybrid nanofibers into ZnO/cellulose nanofibers, then washed with distilled water till the supernatant reached neutral. The hydrolyzed mats were vacuum dried at 50°C for 5 h, and were labeled as ZnO/cellulose-0. Subsequently, they were solvothermally treated in 180°C glycerol bath for 30 and 120 min, respectively, followed by rinsing with distilled water to completely remove glycerol, then vacuum dried at 80°C for 10 h. The final products were nano-ZnO/cellulose hybrid nanofibers. They were coded as ZnO/cellulose-30, and -120, according to the treatment time. The actual content of ZnO in the hybrid nanofibers was measured by calcination of the nanofibers at 500°C in air for 5 h. In this process, the component cellulose would decompose completely to CO_2 and H_2O, whereas ZnO component is remained. The procedure for the preparation of ZnO/cellulose hybrid nanofibers was presented in Scheme 1.

Characterization

Fourier transform infrared (FTIR) spectra were collected on Nicolet Avatar 360 spectrometer (Nicolet, USA) in KBr form. The crystal structure of hybrid nanofiber was characterized by X-ray diffractometer (X'pert MPD Pro, Philips, Netherland) with Cu K_α

radiation ($\lambda = 1.542$ Å). The diameter and morphology of electrospun nanofibers were observed by SEM (JSM-6300LV, JEOL), and TEM (JEM2010, JEOL). All samples were sputter-coated with platinum prior to SEM observation. The fiber diameter was measured using the software SMileView (v2.5, JEOL). About 35 individual nanofibers were measured to obtain the mean value and standard deviation. For TEM measurement, the fibers were dispersed ultrasonically in ethanol before applied onto copper grid. The viscosity molecular weight (M_η) of cellulose component in ZnO/cellulose hybrid nanofibers was determined with cadoxen as the solvent at 25°C by using viscometery according to $[\eta] = 3.85 \times 10^{-2} M_w^{0.76}$ (mL g^{-1}).[29] The solutions were filtered to remove insoluble ZnO particles before measurement.

Photocatalytic activity of ZnO/cellulose hybrid nanofibers

A lab-made photochemical reactor was set up according to our previous work.[24] Five hundred Watt tungsten lamp was used as the visible light source. About 2.0 mg of ZnO/cellulose nanofibrous mats was loaded into a cylindrical glass vessel containing 10 g of 8 mg/L Rhodamine B (RhB) aqueous solution. A light filter was placed between the lamp and dye solution to only allow visible light ($\lambda > 420$ nm) pass through. At time interval of 3, 6, 12, and 24 h, the degradation reaction was ceased and the solution was centrifuged. The RhB concentration in the supernatant was measured on a UV-vis spectrometer (Lambda850, Perkin–Elmer). Three repetitive degradation reactions were conducted for each sample. Only one measurement was made for each batch. After one degradation cycle, the ZnO/cellulose hybrid nanofibrous mats were separated from the reaction medium, washed with distilled water completely, then vacuum dried at 80°C for 10 h. The photocatalytic efficiency of the recycled ZnO/cellulose hybrid nanofibrous mats was tested again according to the same procedure described above. Two control experiments were also conducted to test: (1) the adsorption of RhB on ZnO/cellulose nanofibrous mats in darkness, and (2) photodegradation of RhB when it was exposed to visible light without the presence of ZnO/cellulose hybrid nanofibrous mats.

RESULTS AND DISCUSSION

Morphology of hybrid nanofibers

A typical SEM image of $Zn(OAc)_2$/CA hybrid nanofibers containing 18.2 wt % $Zn(OAc)_2$ is shown in Figure 1(A). The mean fiber diameter of the hybrid nanofibers is 159 ± 28 nm. The fiber topography is relatively smooth without any noticeable bead defects. The TEM image [inset, Fig. 1(A)] of one $Zn(OAc)_2$/CA hybrid nanofiber presents uniform fiber morphology without observable inorganic aggregates within the fiber, suggesting homogeneous dispersion of $Zn(OAc)_2$ in the fiber. This is similar to the appearance of $Zn(OAc)_2$/poly(vinyl alcohol) hybrid nanofibers reported by Hong et al.[25] EDS spectrum [Fig. 1(B)] shows the characteristic L_α X-ray line at 1.01 keV. This can qualitatively confirm the existence of zinc element within the fiber. To get some knowledge about the distribution of $Zn(OAc)_2$ in the hybrid nanofibers, the $Zn(OAc)_2$/CA hybrid nanofibers were immersed in distilled water to wash away $Zn(OAc)_2$. The SEM image of this treated nanofiber is presented in Figure 1(C). From EDS analysis of the whole image area, no X-ray signal was detected for zinc element (not shown here), indicating that this CA nanofiber is $Zn(OAc)_2$ free. The fiber surface becomes relatively rough with obvious elongated concavities (indicated by the arrows). Under the influence of stretching electrical forces, $Zn(OAc)_2$ particles tend to disperse along the fiber axis. This is similar to the distribution of carbon nanotubes[30] and montmorillonite[31] in the inorganic/organic hybrid nanofibers from electrospinning. The removal of those $Zn(OAc)_2$ particles leave grooves behind.

To convert the precursor $Zn(OAc)_2$ in the hybrid nanofibers into ZnO, they were immersed in dilute NaOH aqueous solution. In this process, two reactions took place simultaneously, as described in the following two hydrolysis chemical reactions.[31] As a result, the precursor $Zn(OAc)_2$/CA hybrid nanofibers turned into ZnO/cellulose hybrid nanofibers.

$$\text{Cell} - \text{OCOCH}_3 \xrightarrow{\text{OH}^-} \text{Cellulose} + \text{CH}_3\text{COO}^- \quad (1)$$

$$\text{Zn}(\text{OCOCH}_3)_2 \xrightarrow{\text{OH}^-} \text{ZnO} \downarrow + \text{CH}_3\text{COO}^- \quad (2)$$

Figure 2A shows the FTIR spectra of hybrid nanofibers. The characteristic absorption peak at 1751 ($\nu_{-C=O}$) was presented for CA component in the $Zn(OAc)_2$/CA hybrid nanofibers [Fig. 2(A,a)]. After hydrolysis, the peak at 1751 cm^{-1} disappeared, whereas a new peak at 1640 cm^{-1} (ν_{C-O-C}), and a broader peak at 1080 cm^{-1} (ν_{C-O}) [Fig. 2(A,b)] were shown for cellulose,[32] suggesting that cellulose was regenerated from the hydrolysis of CA [eq. (1)]. In the meantime, the $Zn(OAc)_2$ embedded in the CA nanofibers was transformed into ZnO [eq. (2)]. Compared with precursor nanofibers [Fig. 1(A)], the SEM image of ZnO/cellulose-0 hybrid nanofiber displays very rough surface morphology, many adjacent nanofibers intertwine together [Fig. 2(B)]. Because most precursor $Zn(OAc)_2$ distributes at the near surface layer of $Zn(OAc)_2$/CA hybrid nanofibers [Fig. 1(C)], they readily dissolve upon immersion of the

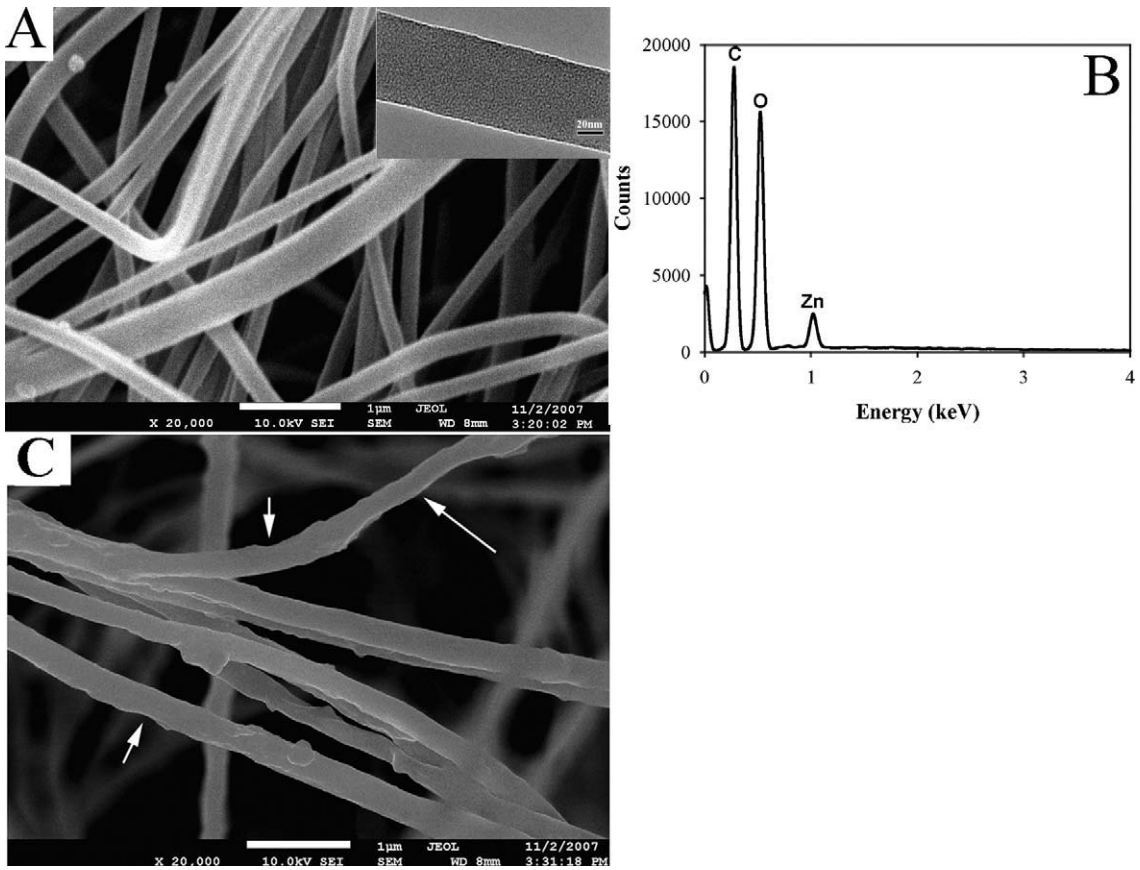

Figure 1 (A) SEM of $Zn(OAc)_2$/CA hybrid nanofibers with $Zn(OAc)_2$ content of 18.2 wt %, inset: TEM of an individual fiber shown in (A); (B) energy dispersive X-ray spectrum of specimen A; and (C) SEM of water washed fibers shown in (A).

hybrid nanofibers in aqueous NaOH solution, OH^- can react with Zn^{2+} to form ZnO colloid precipitates. These precipitates result in rough surfaces of the treated hybrid nanofibers [Fig. 2(B)]. The ZnO colloid precipitates on the adjacent fiber surfaces mix together, causing the many binding sites among fibers.

The ZnO precipitates formed from the hydrolysis of zinc salt at ambient temperature usually do not possess good crystal structure and further hydrothermal

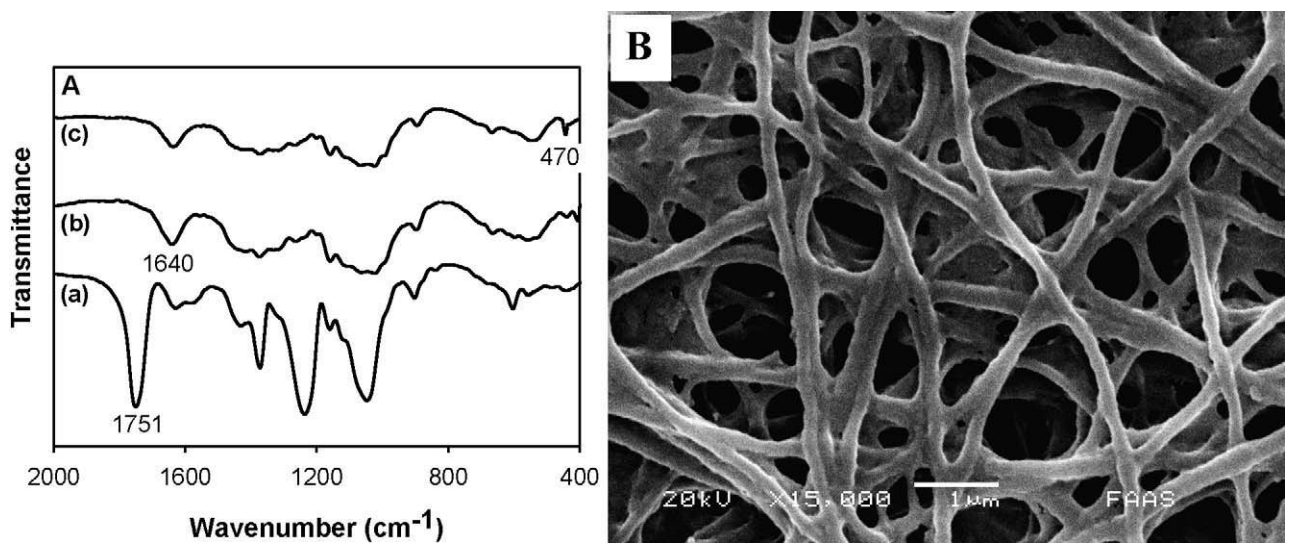

Figure 2 (A) FTIR spectra of hybrid nanofibers: (a) $Zn(OAc)_2$/cellulose acetate, (b) ZnO/cellulose-0 nanofibers, and (c) ZnO/cellulose-120; (B) SEM image of ZnO/cellulose-0 nanofibers.

TABLE I
Viscosity Molecular Weight (M_η) of Cellulose

Sample	Time of hydrothermal treatment (h)	Time of photo irradiation (h)	M_η ($\times 10^{-4}$)
ZnO/cellulose-0	0	0	1.45
ZnO/cellulose-30	0.5	0	1.48
ZnO/cellulose-120	2	0	1.19
ZnO/cellulose-120-a	2	6	1.14
ZnO/cellulose-120-b	2	12	1.10
ZnO/cellulose-120-c	2	24	1.15

treatment is required to induce good crystallization.[33] Therefore in this work, ZnO/cellulose nanofibers were solvothermally treated in glycerol bath at 180°C for various time interval. This process is similar to the preparation of ZnO nanocrystallites through hydrothermal method as reported in the literature.[23] Compared to the ZnO/cellulose-0 nanofibers before solvothermal treatment [Fig. 2(A,b)], FTIR spectrum of ZnO/cellulose-120 nanofibers shows an obvious characteristic peak at 470 cm^{-1} ($\nu_{Zn—O}$) for ZnO [Fig. 2(A,c)], indicating the presence of ZnO crystallites in the hybrid nanofibers.[34] Though cellulose is known to be thermal stable with initial decomposition temperature at $\sim$ 350°C, as determined by thermal gravimetrical analysis,[35] the change of its molecular weight should be a more accurate proof to assess the degradation. Table I lists the M_η of cellulose component in ZnO/cellulose hybrid nanofibers treated for varied time. The M_η of cellulose in ZnO/cellulose-30 displays no difference with that of ZnO/cellulose-0. However, the M_η of cellulose in ZnO/cellulose-120 is 17.9% less than that of ZnO/cellulose-0, due to the possible pyrolysis occurred at 180°C for 120 min. To avoid large loss of mechanical strength and stability of hybrid nanofibers induced by the pyrolysis, prolonged treatment time was not tried further.

Figure 3 shows the TEM images of ZnO/cellulose-120 hybrid nanofibers after solvothermal treatment. ZnO nanoparticles were clearly observed on the fiber surface and in the interior of the fiber. The particles with size of over 25.10 nm are densely resided on the fiber surface [Fig. 3(A)]. This phenomenon was also observed in the preparations of ZnO/PVA nanofibers[25] and of carbon black (CB)/poly(ε-caprolactone) nanofibers.[17] A rod-like ZnO single crystallite with size of 21.91 nm in length and 3.22 nm in width is located $\sim$ 1.5 nm beneath the fiber surface [Fig. 3(A)]. Also the nanoparticles with size of $\sim$ 30 nm in width are sparsely dispersed within the fiber [Fig. 3(B)]. The ZnO nanoparticles in the interior of the hybrid nanofibers proved that precursor $Zn(OAc)_2$ is also distributed inside the $Zn(OAc)_2$/CA nanofibers, besides it is mainly located on the near fiber surfaces. The presence of ZnO nanoparticles within the nanofibers also indicates that the immersion of this precursor fiber into NaOH aqueous solution would allow the solution to permeate into the fiber, then the reaction shown in eq. (2) occurs when OH^- anions meet $Zn(OAc)_2$. Such-formed ZnO colloids are contained in the solid cellulose phase, and therefore they are prohibited from aggregation to form large and dense ZnO precipitates. Thus individual ZnO nanoparticle is formed within the fiber. The reason for the successful penetration of solvent molecules into the fiber is that nanofibers are actually nanoporous materials, as proven by several research groups.[36,37] It is thought that the nanopores are formed by the nucleation and bubbling of solvent vapor in the bulk of the polymer solution in the flying fiber, and most prevalent nanopores are in the order of several nanometers in diameter, and the pores penetrate deep inside the nanofibers.[36]

The HRTEM image [Fig. 3(C)] shows clear lattice fringes without noticeable dislocations and stacking faults, suggesting this ZnO nanoparticle is a defect-free crystal. The *d*-spacing of the lattice fringe is measured to be 0.247 nm, which is in well agreement with the standard d_{101} spacing value. Zhou et al. reported a same *d*-spacing of the crystal ZnO nanorods synthesized at 170°C for 144 h by reacting Zn_3N_2 with NaOH in ethylene glycol solution.[33]

Figure 4 shows the XRD pattern of ZnO/cellulose hybrid nanofibers before and after solvothermal treatment. The broad diffuse scattering peak centered at 18° is attributed to the amorphous phase of cellulose nanofiber.[38] The diffraction peaks in the range of 30–70° on the XRD pattern of hybrid nanofibers (Fig. 4) coincide well with the standard pattern of ZnO (JCPDS 361451), confirming the presence of ZnO in the hybrid nanofibers. For ZnO/cellulose-30 and -120 nanofibers, the peaks corresponding to 102, 110, 103, 112, and 201 planes of ZnO emerge from very weak to strong signals with increasing of treatment time. The strong and resolute diffraction peaks suggest that the as-obtained crystallites can be indexed to hexagonal wurtzite structure of ZnO. Using Bragg equation, the d_{101} spacing of the XRD pattern of ZnO/cellulose-120 is calculated to be 0.247 nm, which is consistent with the measured spacing value from HRTEM image. The intensity of the characteristic peaks of ZnO crystals becomes more pronounced as the solvothermal treatment time was extended from 30 min (ZnO/cellulose-30) to 120 min (ZnO/cellulose-120), indicating that the content or purity of the ZnO hexagonal phase increases with extension of treatment time. For ZnO nanoparticles synthesized from the wet chemical method by reacting zinc salts with bases, the resultant precipitates were usually amorphous and should be further treated through hydrothermal treatment

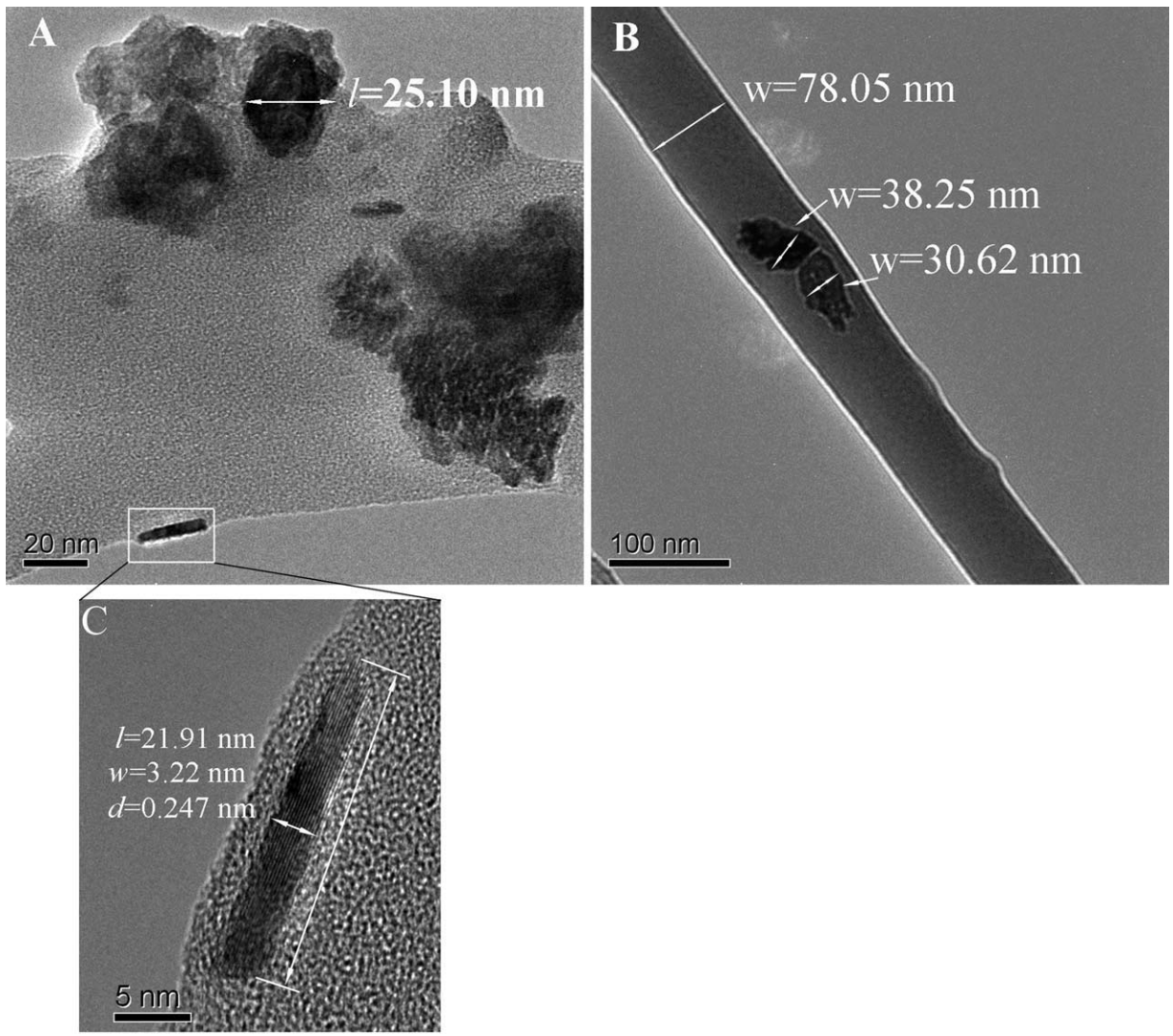

Figure 3 (A) and (B) TEM images, (C) HRTEM images of ZnO/cellulose-120 nanofibers.

or calcination.[39,40] Similar to the effect of these thermal treatment procedures on the formation of ZnO nanoparticles, the solvothermal treatment at 180°C in glycerol readily converts the low crystalline and amorphous ZnO nanoparticles in the hybrid nanofibers to ZnO nanocrystallites.

It is well-known that nano-sized ZnO shows strong photocatalytic decomposition ability toward organic pollutants due to its high photosensitivity and large band gap.[24,41] In this work, we further tested the photocatalytic degradation efficiency of ZnO/cellulose hybrid nanofibers toward RhB. The degradation of RhB catalyzed by ZnO/cellulose hybrid nanofibers under the irradiation of visible light is illustrated in Figure 5. For RhB solution without the presence of hybrid nanofibers, the irradiation caused slow concentration reduction of RhB, and it reached 8.2% over 24 h of irradiation [Fig. 5(A)]. The adsorption of RhB on the hybrid nanofibers was about 2% over 24 h in darkness. The decomposition of RhB with the loading of ZnO/cellulose-30 nanofibers [Fig. 5(B)] was very minor, because these values are close to the sum of the adsorption value of RhB on the fibers and the decomposition value without the loading of catalyst. The ZnO/cellulose-120 showed much stronger catalytic efficiency in degradation of RhB. The degradation rate reached 35.8 and 50.1% after irradiation for 6 and 24 h, respectively, [Fig. 5(C)]. Obviously, the photocatalytic efficiency of the hybrid nanofiber is closely correlated to the crystal structure of ZnO nanoparticles. As shown in Figure 4, the crystallinity of ZnO nanoparticles in the ZnO/cellulose-120 is much higher than that of ZnO/cellulose-30, so the former shows stronger photocatalytic efficiency.

Comparing with the easy aggregation of ZnO nanoparticles and the fragility of ZnO nanofibers in the course of applications,[24] one of the most

important advantages of ZnO/cellulose nanofibers as catalyst is their stable dimension and durability. They are easy to be recycled by separation from the reaction medium. The ZnO/cellulose-120 nanofibers were taken as an example. The recycled hybrid nanofibers still showed acceptable photocatalytic ability, though moderate loss of $\sim$ 10% at corresponding irradiation time was observed for its catalytic efficiency [Fig. 5(D)]. It degraded 29.3 and 42.0% of RhB after irradiation for 6 h and 24 h, respectively. Therefore, the ZnO/cellulose hybrid nanofiber is a type of easy recyclable photocatalyst. It can be potentially used as an effective environmental cleaning material for the photo-degradation of pollutants in water. It should be pointed out that the densely residing ZnO nanoparticles on the outer nanofiber surfaces would certainly play major roles in accepting the photons to generate electron-holes for the oxidative decomposition of RhB molecules, whereas the photocatalytic efficiency of the low content of ZnO nanoparticles residing in the nanofibers is still unknown at this stage. It is possible that the embedded ZnO nanoparticles show minor or even no photocatalytic activity because of the shielding effect of the surrounding cellulose nanofiber matrix. The stability of cellulose matrix under the irradiation of visible light is important for the durability and/or recyclability of ZnO/cellulose hybrid nanofibers. To this end, ZnO/cellulose-120 min was examined as an example. FTIR spectra (not shown here) of this hybrid nanofibers before and after irradiation (for 6, 12, and 24 h) exhibited no new absorption bands except the characteristic bands at 3370 cm^{-1} and 1020–1640 cm^{-1} for cellulose, indicating that the main chemical structure of cellulose did not alter under the applied photocatalytic conditions. The chemical structure stability of cellulose in the TiO_2/cellulose film under the irradiation of simulated natural sunlight ($\sim$ 295–3000 nm) was also demonstrated by Zecchina et al.[42] The M_η of ZnO/cellulose-120 after irradiation for varied time are shown in Table I. No obvious M_η reduction with irradiation time was observed, suggesting that cellulose matrix is photostable within the period tested in this work.

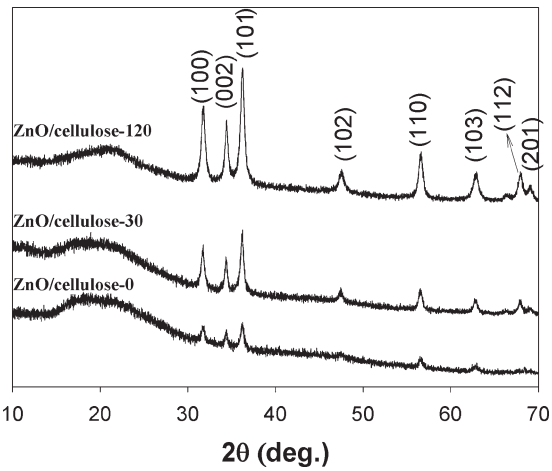

Figure 4 XRD patterns ZnO/cellulose-0, -30, and -120 nanofibers.

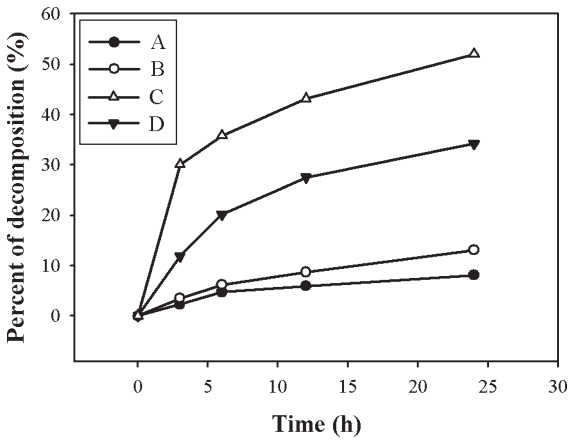

Figure 5 The photocatalytic decomposition percentage of RhB under the irradiation of visible light (A) without the existence of ZnO/cellulose hybrid nanofibers; in the presence of (B) ZnO/cellulose-30 nanofibers; (C) ZnO/cellulose-120 nanofibers; and (D) the second decomposition process using recycled nanofibers from (C).

CONCLUSION

In this work, a new method for the synthesis of ZnO/cellulose hybrid nanofibers was established for the first time. ZnO nanocrystallites were *in situ* grown in cellulose nanofibers through the combination of electrospinning and solvothermal techniques. The solvothermal treatment in glycerol at 180°C for 120 min induced the formation of hexagonal ZnO nanoparticles on and within the nanofibers. This hybrid nanofibers exhibited strong photocatalytic efficiency toward the degradation of RhB. Nearly 50% RhB was decomposed after 24 h of irradiation under visible light using a 500 W tungsten lamp as the light source. This hybrid nanofibrous mats are readily separated from the reaction media by simply using a forceps. The recycled hybrid nanofibrous mats still exhibited photocatalytic capability. Additionally, the cellulose matrix in the hybrid nanofibers is photostable under the applied irradiation conditions. Combining the benefits of ZnO and cellulose, the ZnO/cellulose hybrid nanofibers are a durable, elastic, solvent-resistant, and easy recyclable photocatalyst.

References

1. Kedem, S.; Schmidt, J.; Paz, Y.; Cohen, Y. Langmuir 2005, 21, 5600.

2. Kim, G. M.; Wutzler, A.; Radusch, H. J.; Michler, G. H.; Simon, P.; Sperling, R. A.; Parak, W. J. Chem Mater 2005, 17, 4949.
3. Liu, R. L.; Ye, S. H.; Xiong, X. P.; Liu, H. Q. Mater Chem Phys 2010, 121, 432.
4. Wang, A.; Singh, H.; Hatton, T. A.; Rutledge, G. C. Polymer 2004, 45, 5505.
5. Son, W. K.; Youk, J. H.; Lee, T. S.; Park, W. H. Macromol Rapid Commun 2004, 25, 1632.
6. Mack, J. J.; Viculis, L. M.; Ali, A.; Luoh, R.; Yang, G. L.; Hahn, H. T.; Ko, F. K.; Kaner, R. B. Adv Mater 2005, 17, 77.
7. Lu, X. F.; Zhao, Y. Y.; Wang, C. Adv Mater 2005, 17, 2485.
8. Liang, J. H.; Yang, J. X.; Huang, Y. X.; Liu, H. Q. Acta Chim Sin 2010, 68, 1713.
9. Patel, A. C.; Li, S. X.; Wang, C.; Zhang, W. J.; Wei, Y. Chem Mater 2007, 19, 1231.
10. Liu, R. L.; Huang, Y. X.; Xiao, A. H.; Liu, H. Q. J Alloys Comp 2010, 503, 103.
11. Chronakis, I. S. J Mater Process Technol 2005, 167, 283.
12. Wang, A.; Hsieh, A. J.; Rutledge, G. C. Polymer 2005, 46, 3407.
13. Ge, J. J.; Hou, H. Q.; Li, Q.; Graham, M. J.; Greiner, A; Reneker, D. H.; Harris, F. W.; Cheng, S. Z. D. J Am Chem Soc 2004, 126, 15754.
14. Reneker, D. H.; Yarin, A. L.; Zussman, E.; Xu, H. Adv Appl Mech 2007, 41, 43.
15. Dror, Y.; Salalha, W.; Khalfin, R. L.; Cohen, Y.; Yarin, A. L.; Zussman, E. Langmuir 2003, 19, 7012.
16. Nakane, K.; Yasuda, K.; Ogihara, T.; Ogata, N.; Yamaguchi, S. J Appl Polym Sci 2007, 104, 1232.
17. Tiwari, M. K.; Yarin, A. L.; Megaridis, C. M. J Appl Phys 2008, 103, 044305.
18. Viswanathamurthi, P.; Bhattarai, N.; Kim, H. Y.; Lee, D. R. Nanotechnology 2004, 15, 320.
19. Li, D.; Xia, Y. N. Nano Lett 2003, 3, 555.
20. Madhugiri, S.; Sun, B.; Smirniotis, P. G.; Ferraris, J. P.; Balkus, K. J. Microporous Mesoporous Mater 2004, 69, 77.
21. Sun, Z. C.; Zussman, E.; Yarin, A. L.; Wendorff, J. H.; Greiner, A. Adv Mater 2003, 15, 1929.
22. Cheng, B.; Samulski, E. T. Chem Commun 2004, 8, 986.
23. Wang, J.; Gao, L. J Mater Chem 2003, 13, 2551.
24. Liu, H. Q.; Yang, J. X.; Liang, J. H.; Huang, Y. X.; Tang, C. Y. J Am Ceram Soc 2008, 91, 1287.
25. Hong, Y. L.; Li, D. M.; Zheng, J.; Zou, G. T. Langmuir 2006, 22, 7331.
26. Xu, J. Q. P.; Shun, Y.; Tian, Z. Sensor Actuator B Chem 2000, 66, 277.
27. Sakthivela, S. B. N.; Shankarb, M. V.; Arabindoob, B.; Palanichamyb, M.; Murugesan, V. Sol Energy Mater Sol Cells 2003, 77, 65.
28. Cai, J.; Zhang, L. N.; Zhou, J. P.; Qi, H. S.; Chen, H.; Kondo, T.; Chen, X. M.; Chu, B. Adv Mater 2007, 19, 821.
29. Brown, W.; Wiskston, R. Eur Polym Mater 1965, 1, 1.
30. Hou, H. Q.; Ge, J. J.; Zeng, J.; Li, Q.; Reneker, D. H.; Greiner, A.; Cheng, S. Z. D. Chem Mater 2005, 17, 967.
31. Fong, H.; Liu, W. D.; Wang, C. S.; Vaia, R. A. Polymer 2002, 43, 775.
32. Liu, H. Q.; Hsieh, Y. L. J Polym Sci Part B: Polym Phys 2002, 40, 2119.
33. Wei, M. D.; Qi, Z. M.; Ichihara, M.; Honma, I.; Zhou, H. S. Nanotechnology 2007, 18, 095608.
34. Wu, H.; Pan, W. J Am Ceram Soc 2006, 89, 699.
35. Liu, S. L.; Zhang, L. N.; Zhou, J. P.; Xiang, J. F.; Sun, J. T.; Guan, J. G. Chem Mater 2008, 20, 3623.
36. Srikar, R.; Yarin, A. L.; Megaridis, C. M.; Bazilevsky, A. V.; Kelley, E. Langmuir 2008, 24, 965.
37. Casper, C. L.; Stephens, J. S.; Tassi, N. G.; Chase, D. B.; Rabolt, J. F. Macromolecules 2004, 37, 573.
38. Kim, C. W.; Frey, M. W.; Marquez, M.; Joo, Y. L. J Polym Sci Part B: Polym Phys 2005, 43, 1673.
39. Liu, B.; Zeng, H. C. J Am Chem Soc 2003, 125, 4430.
40. Carnes, C. L.; Klabunde, K. J. Langmuir 2000, 16, 3764.
41. Daniele, S.; Ghazzal, M. N.; Hubert-Pfalzgraf, L. G.; Duchamp, C.; Guillard, C.; Ledoux, G. Mater Res Bull 2006, 41, 2210.
42. Uddin, M. J.; Cesano, F.; Bonino, F.; Bordiga, S.; Spoto, G.; Scarano, D.; Zecchina, A. J Photochem Photobiol A 2007, 189, 286.